의학석사 학위논문

The study for characterization and integrin $\alpha_v\beta_3$ targeting of ^{64}Cu-cRGDyK-HSA

방사성구리-cRGDyK-알부민을 이용한 인테그린 $\alpha_v\beta_3$ 표적화 및 특성에 관한 연구

2016 년 2 월

서울대학교 대학원

협동과정 중양생물학 전공

박 초 롱

A thesis of the Master's degree

방사성구리-cRGDyK-알부민을 이용한 인테그린 $\alpha_V\beta_3$ 표적화 및 특성에 관한 연구

The study for characterization and integrin$\alpha_V\beta_3$ targeting of ^{64}Cu-cRGDyK-HSA

February 2016

Interdisciplinary Program in Tumor Biology,

Seoul National University

College of Medicine

Cho Rong Park

ABSTRACT

Cho Rong Park

Interdisciplinary Program in Tumor Biology

The Graduate School

Seoul National University

Introduction: RGD is famous integrin $\alpha_V\beta_3$ targeting peptide, so integrin $\alpha_V\beta_3$ targeting for tumor imaging is useful for tumor imaging. However, RGD has the short circulation time and the majority of the injected probes are cleared through the renal system or hepatobiliary system. To enhance the half-lives of RGD and tumor targeting, cRGDyK was conjugated to HSA via bioorthogonal click reaction. To develop the best RGD conjugated HSA nanoparticles, two types of cRGDyK conjugated HSA were synthesized and the probes (cRGDyK-HSA) were characterized, radiolabeled and preliminarily tested in *in vitro* and *in vivo* properties of integrin $\alpha_V\beta_3$ expressing cancer targeting.

Methods: HSA was conjugated with DBCO-NHS ester (molar ratio of HSA : DBCO-NHS ester; 1 : 5.62 for reaction 1 and 1 : 11.24 for reaction 2) for click reaction linker. And DBCO-HSA was conjugated with N_3-cRGDyK (HSA-DBCO : N3-cRGDyK; 1 : 3 for reaction 1 and 1 : 6 for reaction 2). For radiolabeling, ^{64}Cu-labeled 3-azidopropyl-NOTA was conjugated to DBCO-HSA and cRGDyK-HSA via click reaction. At each conjugation step, the conjugates were purified using PD-10 column, eluted with the PBS buffer. All conjugation products were analyzed via MALDI-TOF-MS and radiolabeling efficiencies were measured by instant thin layer chromatography (ITLC). The stability of ^{64}Cu-labeled HSA and -cRGDyK-HSA in serum were monitored during 48 hrs. To certify cRGDyK-HSA binding to integrin $\alpha_v\beta_3$ in cell level, FNR648-labeled cRGDyK-HSA was used for confocal microscopy imaging. ^{64}Cu-labeled HSA and -cRGDyK-HSA were intravenously injected to SK-OV3 tumor bearing mice and the distribution of the probes in mice were imaged by small animal PET at 10 min, 4 hours, 24 hours and 48 hours post injection (p.i.)..

Results: DBCO-NHS ester and cRGDyK were successfully conjugated to HSA, according to their molar ratio. In case of DBCO, the number of DBCO conjugated to HSA; reaction 1 was 3.94 ± 0.70 and reaction 2 was 6.72 ± 0.41. In case of cRGDyK, the number of cRGDyK conjugated to DBCO-HSA; reaction 1 was 2.07 ± 0.51 and reaction 2 was 5.29 ± 0.76. Radiolabeling efficiencies of ^{64}Cu-HSA and ^{64}Cu-cRGDyK-HSA (reaction 2) was 100% and after PD-10 purification, that of ^{64}Cu-cRGDyK-HSA (reaction 1) was almost 100%. ^{64}Cu-HSA and -cRGDyK-HSA were stable in serum after 48 hours incubation. Confocal microscopy images showed that FNR648-labeled cRGDyK-HSA were localized in cell membrane and intracellular regions, this localization in cells was blocked when cells were pre-incubated with excess cRGDyK. The cell uptake of ^{64}Cu-labeled cRGDyK-HSA (reaction 1 and reaction 2) was higher in SK-OV3 cells (integrin $\alpha_V\beta_3$ positive) than 22Rv1 cells (integrin $\alpha_V\beta_3$ negative, $P < 0.05$). PET images revealed that reaction 2 of cRGDyK-conjugated HSA had the highest uptake in tumor (5.37 ± 1.09 %ID/g).

Conclusion: DBCO-HSA and cRGDyK-HSA were successfully synthesized. As the molar ratio of DBCO or cRGDyK were different, the number of attached DBCO or cRGDyK to HSA were consistently different. Using click reaction, ^{64}Cu was successfully labeled to HSA and cRGDyK-HSA. cRGDyK-HSA could bind integrin $\alpha_V\beta_3$ in tumor cells and *in vivo* PET imaging results probed that the ^{64}Cu-cRGDyK-HSA could target tumor after 4 hours p.i.. These results demonstrate that ^{64}Cu-labeled cRGDyK-HSA can be used as PET tumor imaging probes.

Keywords: integrin $\alpha_V\beta_3$, RGD, Human serum albumin (HSA), bioorthogonal click reaction, PET imaging, ^{64}Cu

Student number: 2014-21152

CONTENTS

LIST OF TABLES AND FIGURES

LIST OF ABBREVIATIONS

RGD, Arg-Gly-Asp

HSA, Human Serum Albumin

cRGDyK, cyclic Arg-Gly-Asp-D-Tyr-Lys

DBCO-NHS, dibenzocyclooctyl-NHS

MALDI-TOF, Matrix Assisted Laser Desorption/Ionization-Time Of Flight

NOTA, 1,4,7-triaza-cyclononane-1,4,7-triacetic acid

ITLC-SG, Instant Thin Layer Chromatography-Silica Gel

FBS, Fetal Bovine Serum

RT-PCR, Reverse Transcriptase-Polymerase Chain Reaction

HBSS, Hank's Balanced Salt Solution

BSA, Bovine Serum Albumin

PET, Positron Emission Tomography

%ID/g, % Injected Dose/gram

INTRODUCTION

Integrin $\alpha_V\beta_3$ targeting for tumor imaging

For the expansion of a tumor mass, new blood vessel formation is important. Angiogenesis is regulated through the balance of pro-angiogenic and anti-angiogenic processes and when pro-angiogenic processes are dominant, angiogenesis occurs (1, 2, 4). Because angiogenesis depends on the adhesive interaction of vascular cells, adhesive receptor integrin $\alpha_V\beta_3$ was identified and known as angiogenic marker. RGD (Arg-Gly-Asp) is famous integrin $\alpha_V\beta_3$ targeting peptide, which was identified from finding the cell attachment activity of fibronectin (5, 6). For selectively targeting to integrin $\alpha_V\beta_3$ and improving affinity, many modified RGD peptides are found (7). Many research groups are already using RGD or modified RGD peptides for tumor targeting (8-10). Because integrin $\alpha_V\beta_3$ is already well known about the angiogenesis aspect during tumor mass expansion and there are many molecules can target

integrin $\alpha_v\beta_3$, so integrin $\alpha_v\beta_3$ targeting for tumor imaging is very useful for tumor imaging.

HSA as a carrier

Human serum albumin (HSA) is molecular weight of 65.5kDa and the major soluble protein in circulating system, a blood concentration is about 50 mg/mL (11). Because HSA has long half-life (an average half-life is 19 days) and already exists in body, many HSA-based nanoparticles are developed. The most famous one is ABI 007 (Abraxane ®), which was approved by the FDA in 2005, already used in clinical trials (12-14). Paclitaxel has bad solubility in water, as the drug were incorporated in albumin, the solubility and toxicity problem are improved.

As mentioned before, there are many kinds of RGD-based peptides. But RGD has the short circulation time and the majority of the injected probes are cleared through the renal system (9) or hepatobiliary system (15). As the imaging moiety, fast clearance is a good aspect for tumor imaging, but as the

therapy aspects, particles should be incorporated to tumor for a long time to cure the tumor. And when using with radionuclide labeled RGD sequences for therapy, because the radionuclide for therapy emits high energy, high uptake in kidney may cause kidney damages (16, 17). To solve this problem, HSA can be an answer to improve longer circulation in body. With prolonged circulation time in blood, we can also expect more accumulation of the probes to tumors.

Click reactions for conjugation

Click reactions have broad meaning, which meet being selective, high yielding, and having good reaction kinetics. At the early time, copper-catalyzed azide–alkyne cycloaddition was called “click” chemistry. But in these days, researchers are started to focus on bioorthogonal click reaction, which are inert to biological environments (18). Because this reaction doesn’t need exogenous metal catalysts, which can cause mild to severe cytotoxic effects, it is good for making nanoparticles to use *in vivo* (19).

Purpose of this study

RGD peptides have been used as tumor imaging to target angiogenesis for a long times, but fast-clearance via kidney is problematic. Conjugating RGD peptides to HSA via bioorthogonal click reaction, which can conduct the conjugating reaction in favorable condition, I wanted to enhance the half-lives of RGD in *in vivo* and the targeting capacity of RGD. To develop the best RGD conjugated HSA nanoparticles, I synthesized two types of cRGDyK (cyclic Arg-Gly-Asp-D-Tyr-Lys) conjugated HSA using click reaction. Then the probes (cRGDyK-HSA) were characterized, radiolabeled with ^{64}Cu and tested in *in vitro* and *in vivo* level whether this probes can be used or not.

MATERIALS AND METHODS

Conjugation of HSA with DBCO and cRGDyK

First, HSA (5 mg) was conjugated with dibenzocyclooctyl-NHS ester (DBCO-NHS ester, 40 mg/mL, dissolved in DMSO) in 1 mL of phosphate-buffered saline (PBS, pH 7.4) in two molar ratio of 1 : 5.62 and 1 : 11.24 for 30 min at 37℃. Two types of DBCO-HSA conjugates were then purified using PD-10 column (GE Healthcare, Little Chalfont, Buckinghamshire, UK) and eluted with the same PBS buffer. The purified DBCO-HSA were then reacted with azido cyclic RGDyK (N_3-cRGDyK, 1.4 mg/mL, dissolved in PBS) in 1mL of PBS in two molar ratio of 1 : 3 and 1 : 6 for 30 min at 37℃. Both of HSA-cRGDyK conjugates were further purified using the PD-10 column and eluted with PBS buffer. In each step, the protein concentration was measured by the bicinchoninic acid (BCA) protein assay kit (Pierce Endogen, Rockford, IL, U.S.A), and the samples were analyzed via MALDI TOF-TOF 5800 System (AB SCIEX, Framingham, MA, U.S.A) in every conjugation step.

Radiolabeling of DBCO-HSA and cRGDyK-HSA

The total volume of ^{64}Cu was reduced with N_2 gas, the pH was adjusted to 4.5 using 1 M sodium acetate buffer (NaOAc, pH 5.4). 3-azidopropyl-NOTA (3-azidopropyl-1,4,7-triaza-cyclononane-1,4,7-trizcetic acid, 16 nmole dissolved in 10 μL D.W) was added pH adjusted $^{64}CuCl_2$. The reaction mixture was incubated at 50℃ for 10 minutes in heating block. After ^{64}Cu labeling to 3-azidopropyl-NOTA, 3-azidopropyl-^{64}Cu was added to DBCO-HSA or cRGDyK-HSA at 37℃ for 30 minutes in heating block. To improve the radiolabeling efficiency, 3-azidopropyl-^{64}Cu added cRGDyK-HSA were incubated in 4℃ for 16 hours at shaker. Two types of DBCO-HSA and cRGDyK-HSA conjugates were purified using PD-10 column and eluted with PBS buffer. In each step, the labeling efficiency of products (3-azidopropyl-NOTA with ^{64}Cu or 3-azidopropyl-^{64}Cu with DBCO-HSA or cRGDyK-HSA) was determined using Instant Thin Layer Chromatography (ITLC-SG) with 0.1 M citric acid as the solvent. The strip was counted by Bio-

Scan AR-2000 System imaging scanner (Bio-Scan Inc., Washington D.C, U.S.A).

Serum stability test

Human serum was filtered with Minisart syringe filter, hydrophilic (0.2 ㎛, Sartorius stedim biotech., Bohemia, NY, U.S.A) and 5ml syringe (BD, Franklin Lakes, NJ, U.S.A). Filtered human serum was mixed with ^{64}Cu-labeled HSA or -cRGDyK-HSA and incubated 37℃ shaking incubator. At each time points (10 minutes, 4 hours, 24 hours, 48 hours after the probes mixed with human serum), the mixture were analyzed using ITLC-SG with 0.1 M citric acid as the solvent. The strip was counted by Bio-Scan AR-2000 System imaging scanner.

Cell culture

The human cancer cell lines, SK-OV3(ovarian cancer), PC3, DU145, 22Rv1(prostate cancer) and KB(head and neck cancer) were grown in RPMI

medium (Welgene, Daegu, South Korea) containing 10% (v/v) fetal bovine serum (FBS, Invitrogen, Grand Island, NY, U.S.A) and 1% antibiotics (Invitrogen, Grand Island, NY, U.S.A). Cells were incubated in a 37℃ humidified incubator with 5% CO_2 atmosphere.

Reverse Transcriptase-Polymerase Chain Reaction (RT-PCR)

Total RNA were obtained from cells (SK-OV3, PC3, DU145, 22Rv1 and KB) with the Trizol reagent (Invitrogen, Carlsbad, CA, U.S.A). For cDNA synthesis, amfiRivert Platinum cDNA synthesis Master Mix (GenDEPOT, Barker, TX, U.S.A) was used with 2 ug of mRNA following the manufacturer's instructions. From synthesized cDNA, the mRNA expression level of integrin α_v, β_3 and β-actin were detected. The sequences of the forward and reverse primers of integrin α_v were 5'-GAA AAG AAT GAC ACG GTT GC and 5'-TAA CCA ATG TGG AGT TGG TG, which give product size of 318

base pairs. The sequences of the forward and reverse primers of integrin β_3 were 5'-CAG ACT TGG GCA GGG TAC AG and 5'-GAC CTT CAA GAC TGG CTG CT, which give product size of 396 base pairs. The sequences of the forward and reverse primers of β-actin were 5'-ACC AGG GCT GCT TTT AAC TCT and 5'-GAG TCC TTC CAC GAT ACC AAA. The PCR was run after an initial single cycle of 94℃ for 5 minutes. After initial single cycle, there is 30 cycles of following procedure; 94℃ for 30 seconds, annealing temperature for 1 minutes and 72℃ for 10 minutes. The annealing temperature of integrin α_v is 62℃, integrin β_3 is 58℃ and β-actin is 58℃. In the last step, 72℃ for 10 minutes. After amplification, PCR products were analyzed by gel electrophoresis in 1.2% agarose gels and visualized with Loading star (DyneBio Inc, Seoul, Korea) staining.

Western blotting

Total proteins were isolated from cells (SK-OV3, PC3, DU145, 22Rv1 and KB) using radio-immunoprecipitation assay (RIPA) buffer (Sigma, St. Louis, MO, U.S.A) and protease inhibitor (Roche, Nutley, NJ, Switzerland). Lysates were cleared by centrifugation at 15,000 rpm at 4°C. Total proteins were quantified by BCA protein assay kit. Lysate of each cell sample (20 μg) mixed with 4× polyacrylamide gel electrophoresis sample buffer (Invitrogen, Grand Island, NY, U.S.A) was loaded onto 8% SDS-PAGE gel. After gel electrophoresis, the gels were blotted onto PVDF membranes (Millipore, Watford, UK). The PVDF membranes were blocked with 5% skim milk in Tris-Buffered Saline – Tween-20 buffer (20mM Tris, 138mM NaCl and 0.1% Tween-20, TBS-T) for 1 hour at room temperature. The membranes were incubated overnight at 4℃ with primary antibodies for integrin α_v (sc-9969, Santa Cruz, Dallas, Texas, U.S.A; diluted 1:200), integrin β_3 (#13166, Cell signaling, Danvers, MA, U.S.A; diluted 1:1000) and β-actin (A5441, Sigma-Aldrich, St. Louis, MO, U.S.A; diluted 1:5000). Membrane were then probed

with HRP conjugated anti-rabbit or anti-mouse IgG (Cell Signaling Technology, Danvers, MA, U.S.A). Visualization was performed using the ECL reagents (Roche, Nutley, NJ, U.S.A). The signal intensity was measured using an LAS-3000 imaging system (Fujifilm, Tokyo, Japan).

Confocal microscopy

For immunofluorescence analysis in cancer cells, 1.5×10^5 cells (SK-OV3) were seeded in each well of 12-well plate (Nalge NUNC International, Naperville, IL, U.S.A) since the day before. For staining, all procedures did 1% BSA (g/v) containing Hank's Balanced Salt Solution (HBSS, Invitrogen, Grand Island, NY, U.S.A). For cold cRGDyK blocking group, the cells were blocked for 30 minutes with 500-fold higher deprotected cRGDyK (Futurechem, Seoul, South Korea) in 1% BSA containing HBSS. For cold HSA blocking group, the cells were blocked for 30 minutes with 1000nmole HSA (500 fold higher) in 1% BSA containing HBSS. Cells were incubated with 2 nmole of FNR648-labeled HSA or cRGDyK-HSA for 30 minutes. Cells were

washed three times with PBS. After staining, the slides were mounted with Prolong Gold reagent (Invitrogen, Grand Island, NY, U.S.A). Fluorescence images were taken by confocal laser scanning microscope (Leica TCS SP8, Wetzlar, Hesse, Germany).

In vitro cell uptake assay

The 22Rv1 and SK-OV3 cells were split 4×10^6 cells per 5mL test tube and cells were washed once with PBS. All cells in test tubes were treated with the ^{64}Cu-labeled HSA or cRGDyK-HSA (74000 Bq per tube) in 0.2 mL of 1% BSA (g/v) containing HBSS for 1 hours in 37℃ shaking incubator. The cells were washed two times with cold PBS and lysed in 0.3 mL 1% SDS. The radioactivity of the cells was counted using a PerkinElmer 1470 automatic γ-counter (PerkinElmer, Waltham, Massachusetts, U.S.A).

Animal modeling and PET imaging

All animal studies were performed under approval from the Seoul National University Institutional Animal Care and Use Committee (IACUC). BALB/c nude mice (5 week-old, female) were purchased from the Orient Bio Inc., (Seongnam, South Korea). Ovarian cancer cell line, SK-OV3 (4×10^6) was subcutaneously injected into right lower flanks. Tumors were grown to a size of 5 – 10 mm in diameter (3 - 4 weeks). The tumor-bearing mice were subjected to PET imaging studies.

Small animal PET imaging of tumor-bearing mice was performed using PET box (SOFIE Bioscience, Culver, CA, U.S.A). SK-OV3 tumor bearing mice were injected with 0.37–0.74 MBq (1.5-3 nmole for ^{64}Cu-HSA; 3.5–3.8 nmole for ^{64}Cu-cRGDyK-HSA) of ^{64}Cu-HSA or ^{64}Cu-cRGDyK-HSA via tail vein. At various times after injection of probes (10 minutes, 4, 24, 48 hours), the mice were anesthetized with 2% isoflurane and placed in the prone position. Static scans (10 minutes scans for 10 min, 4 hours after injection; 20 minutes scans for 24, 48 hours after injection) were obtained and the images

were reconstructed by AMIDE algorithm. Reconstructed data from PET box were visualized and co-registered using InVivoScope (Bioscan, Washington D.C, WA, U.S.A).

RESULTS

Characterization of DBCO-HSA and cRGDyK-HSA

Figure 1. shows the procedure to make DBCO-HSA and cRGDyK-HSA. To confirm how many DBCO or cRGDyK were conjugated to HSA, MALDI-TOF analysis was conducted in each conjugation steps. The molecular weight of all reaction products shown in Table 1. The number of conjugated DBCO in HSA was 3.94 ± 0.70 in reaction 1 (reaction ratio of HSA : DBCO-NHS ester was 1 : 5.62) and 6.72 ± 0.41 in reaction 2 (reaction molar ration of HSA : DBCO-NHS ester was 1 : 11.24). Each of DBCO-HSA (reaction 1 and reaction 2) was further conjugated with N_3-cRGDyK via copper-free azide-alkyne cycloaddition. The number of conjugated cRGDyK in DBCO-HSA also certified by MALDI-TOF analysis, which was 2.07 ± 0.51 in reaction 1 cRGDyK-HSA (reaction 1, reaction molar ratio of DBCO-HSA : N_3-cRGDyK was 1 : 3) and 5.29 ± 0.76 in reaction 2 cRGDyK-HSA(reaction 2, reaction molar ratio of DBCO-HSA : N_3-cRGDyK was 1 : 6).

A

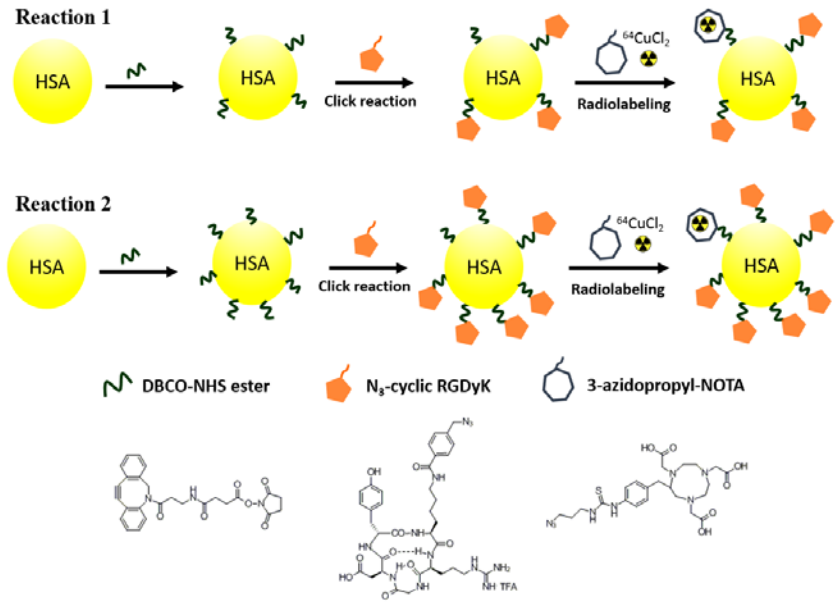
Reaction 1
HSA
HSA
Click reaction
HSA
$^{64}CuCl_2$
Radiolabeling
HSA
Reaction 2
HSA
HSA
Click reaction
HSA
$^{64}CuCl_2$
Radiolabeling
HSA
DBCO-NHS ester
N_3-cyclic RGDyK
3-azidopropyl-NOTA

B

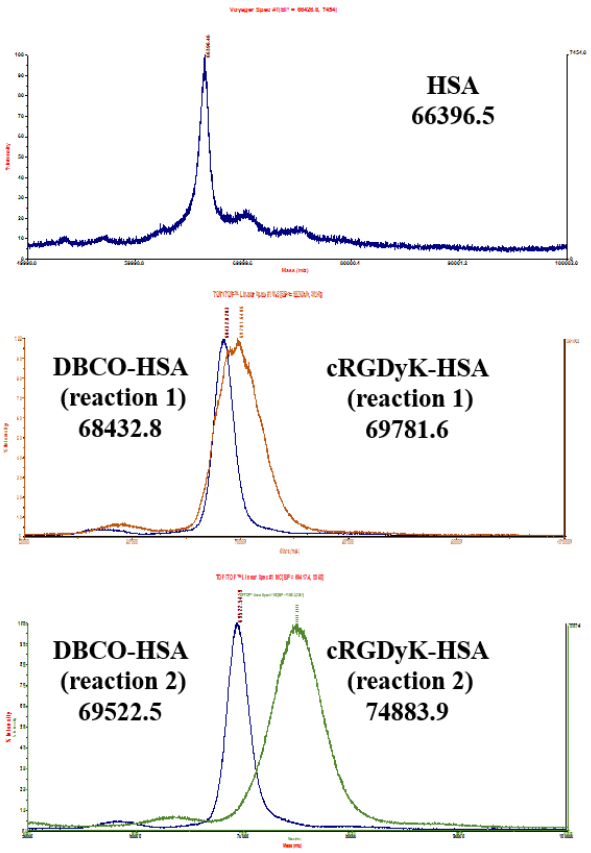
HSA
66396.5
DBCO-HSA
(reaction 1)
68432.8
cRGDyK-HSA
(reaction 1)
69781.6
DBCO-HSA
(reaction 2)
69522.5
cRGDyK-HSA
(reaction 2)
74883.9

Figure 1. Characterization of DBCO-HSA and cRGDyK-HSA

(A) Diagram of procedure to conjugate DBCO, cRGDyK or ^{64}Cu to HSA. First, DBCO was conjugated to HSA. Using this DBCO, N_3-cRGDyK or 3-azidopropyl-NOTA was conjugated to HSA via azide-alkyne cycloaddition. The difference between reaction 1 and reaction 2 is the number of DBCO or cRGDyK (The number of DBCO or cRGDyK is on Table 1). (B) The representative MALDI-TOF analysis results. The number is molecular weight. As HSA was conjugated to DBCO or cRGDyK, the molecular weight was increased.

Table 1. Investigation of molecular mass using MALDI-TOF and analysis of MALDI-TOF data

	Molecular weight	**(− HSA molecular weight)**	**DBCO molar ratio**
DBCO-HSA (reaction 1)	68164.33 ± 332.08	1864.33 ± 332.08	3.94 ± 0.70
DBCO-HSA (reaction 2)	69484.14 ± 194.25	3184.14 ± 194.25	6.72 ± 0.41
	Molecular weight	**(− DBCO-HSA molecular weight)**	**cRGDyK molar ratio**
cRGDyK-HSA (reaction 1)	70014.09 ± 434.08	1849.77 ± 458.22	2.07 ± 0.51
cRGDyK-HSA (reaction 2)	74210.17 ± 824.49	4726.03 ± 675.11	5.29 ± 0.76

Data are expressed as means ± SDs of three independent experiments.

Molecular mass was measured using MALDI-TOF and the number of DBCO or cRGDyK was calculated as follows;

(Molecular weight of HSA is 66300, DBCO-NHS-ester is 473.48, N_3-cRGDyK is 892.69)

$$\text{DBCO molar ratio} = \frac{(\,Molecular\ weight\ of\ MALDI-TOF\,) - (\,molecular\ weight\ of\ HSA\,)}{(\,molecular\ weight\ of\ DBCO-NHS\ ester\,)}$$

$$\text{cRGDyK molar ratio} = \frac{(\,Molecular\ weight\ of\ MALDI-TOF\,) - (\,molecular\ weight\ of\ HSA\,)}{(\,molecular\ weight\ of\ N_3-cRGDyK\,)}$$

Radiolabeling efficiency and stability of DBCO-HSA and cRGDyK-HSA

For quantitative *in vitro* and *in vivo* study, DBCO-HSA (reaction 1 and reaction 2) and cRGDyK-HSA (reaction 1 and reaction 2) were radiolabeled with ^{64}Cu. Radiolabeling efficiencies were analyzed by ITLC-SG with 0.1 M citric acid as a solvent at each step; free $^{64}CuCl_2$ reached up to Rf =1.0 (retention factor), ^{64}Cu-3-azidopropyl goes up to Rf=0.7 and ^{64}Cu-HSA or ^{64}Cu-cRGDyK-HSA remained at the origin (Rf=0.0). For using azide-alkyne cycloaddition, at first, 3-azidopropyl-NOTA was radiolabeled with ^{64}Cu in 50℃ for 10 minutes at heat block. ^{64}Cu-labeled 3-azidopropyl had only one peak at Rf=0.7 in ITLC-SG, so 3-azidopropyl-NOTA was well radiolabeled with ^{64}Cu (Figure 2A). ^{64}Cu-labeled 3-azidopropyl was then added to DBCO-HSA (reaction 1 and reaction 2) and cRGDyK-HSA (reaction 1 and reaction 2) in 37℃, 30 minutes for azide-alkyne reaction. In Figure 2B, both of ^{64}Cu-3-azidopropyl added DBCO-HSA (reaction 1 and reaction 2) successfully radiolabeled with ^{64}Cu (Rf=0.0). In case of cRGDyK-HSA, radiolabeling

efficiency was 27% for reaction 1 and almost 100% for reaction 2 (Figure 2C). So, cRGDyK-HSA in reaction 2 were successfully radiolabeled as DBCO-HSA. For further enhancing the radiolabeling efficiency of cRGDyK-HSA in reaction 1, ^{64}Cu-labeled 3-azidopropyl added cRGDyK-HSA (reaction 1) was incubated in 4℃ for 16 hours at shaker. After the incubation at 4℃, the radiolabeling efficiency of ^{64}Cu-3-azidopropyl added cRGDyK-HSA (reaction 1) was increased (78%, Figure 2C). To purify the ^{64}Cu-HSA or -cRGDyK-HSA, all products were purified by PD-10 column. After the purification procedure, all of the radiolabeling efficiency of ^{64}Cu-HSA or -cRGDyK-HSA (reaction 1 and reaction 2) were 100% (Rf=0.0, Figure 2B, 2C). After the PD-10 purification, ^{64}Cu-cRGDyK-HSA (reaction 1) can be used as the imaging probe for PET imaging.

To certify the stability of ^{64}Cu-HSA and ^{64}Cu-cRGDyK-HSA (in each type; reaction 1 and reaction 2) were mixed with filtered human serum in 37℃ shaking incubator. As time goes on, ^{64}Cu-HSA or ^{64}Cu-cRGDyK-HSA (reaction 1 and reaction 2) remained at the origin (Rf=0.0) and there were no

^{64}Cu-labeled 3-azidopropyl or free ^{64}Cu. So, the ^{64}Cu-labeled HSA or cRGDyK-HSA were stable in human serum after 48 hours.

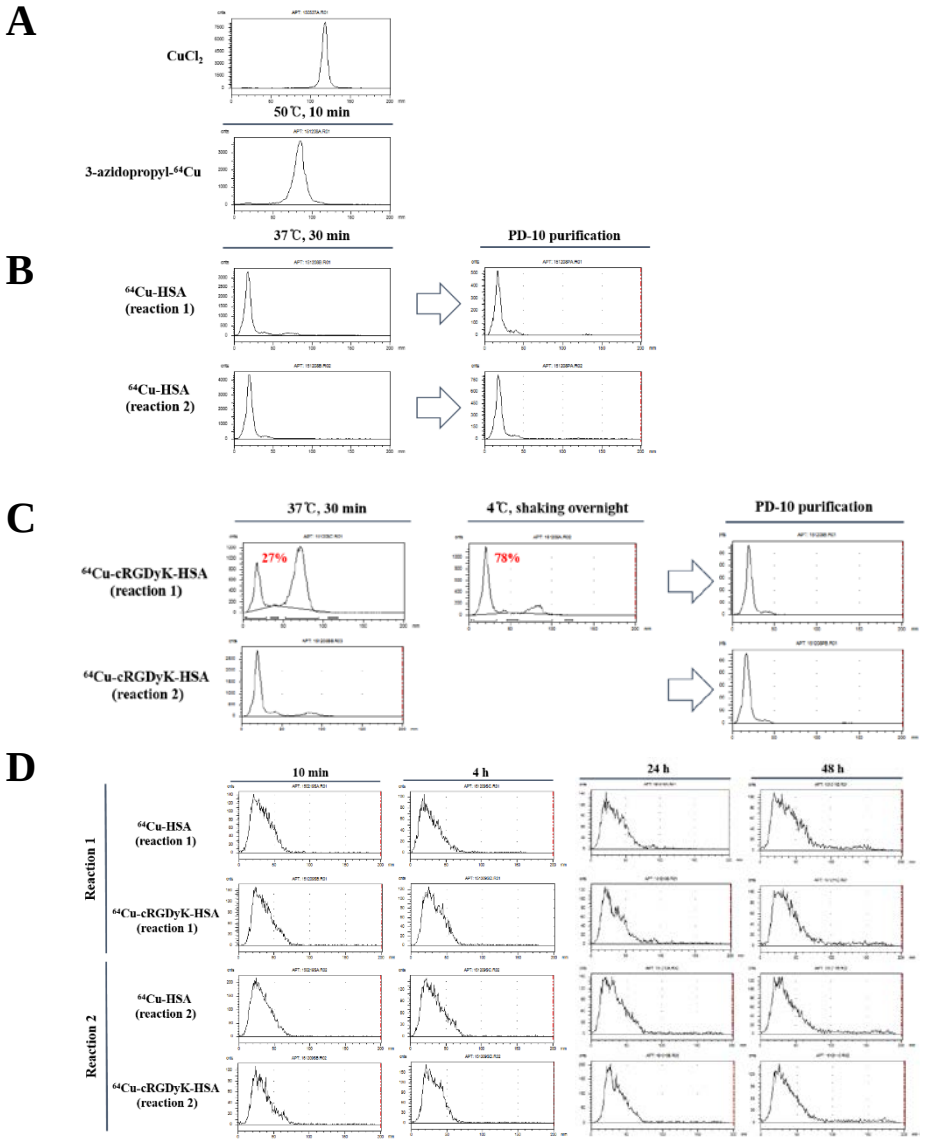

Figure 2. Labeling efficiency and stability of ^{64}Cu-HSA and -cRGDyK-HSA

(A) ITLC-SG data of $^{64}CuCl_2$ and 3-azidopropyl-^{64}Cu at 0.1 M citric acid. $^{64}CuCl_2$ was at Rf=1.0 and 3-azidopropyl-^{64}Cu was at Rf=0.7. (B) ^{64}Cu-HSA (reaction 1 and reaction 2) were labeled at 37℃ for 30 minutes in heating block.

Labeled ^{64}Cu-HSA was at the origin (Rf=0.0). After reaction, ^{64}Cu-HSA (reaction 1 and reaction 2) were purified with PD-10 column. (C) ^{64}Cu-cRGDyK-HSA(reaction 1 and reaction 2) were also labeled at 37℃ for 30 minutes in heating block. Labeled ^{64}Cu-cRGDyK-HSA was at Rf=0.0. For further labeling reaction, after the 37℃ for 30 minutes reaction, 4℃ for overnight (16 hours) shaking reaction was added to reaction 1. After reaction, ^{64}Cu-cRGDyK-HSA (reaction 1 and reaction 2) were purified with PD-10 column. At each step, the labeling efficiency of ^{64}Cu-HSA and -cRGDyK-HSA were detected in ITLC-SG at 0.1 M citric acid as the solvent. (D) Serum stability test of ^{64}Cu-HSA and -cRGDyK-HSA (reaction 1 and reaction 2). The stability of ^{64}Cu-HSA and –cRGDyK-HSA were detected in ITLC-SG, eluted with 0.1 M citric acid.

Integrin $\alpha_V\beta_3$ expression in cancer cell lines

To select a integrin $\alpha_V\beta_3$ positive cell lines, integrin $\alpha_V\beta_3$ mRNA and protein expression levels in some cancer cell lines were confirmed using RT-PCR and western blot (Figure 3A, B) RT-PCR data showed that the mRNA expression levels of integrin α_V were very similar, but the integrin β_3 mRNA was only expressed in PC3, DU145, SK-OV3 cells (Figure 3A). In a case of western blotting data, integrin α_V was also expressed in all cell lines as protein level, but integrin β_3 was only expressed in DU145, SK-OV3 cells (Figure 3B). According to the mRNA expression (RT-PCR) and protein expression (western blot) results, SK-OV3 was the highest integrin $\alpha_V\beta_3$ expressing cell in all compared cells (KB, 22Rv1, PC3, DU145, SK-OV3).

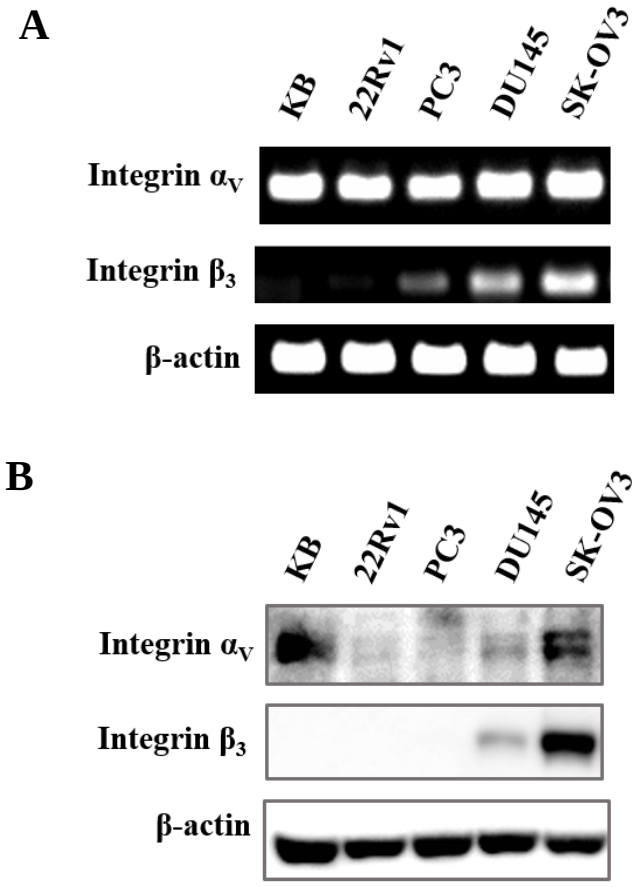

Figure 3. Screening for the integrin $\alpha_V\beta_3$ expressing cell line

(A) RT-PCR for mRNA expression level analysis. The 319-bp fragments of α_V mRNA were detected at all cell lines, and 396-bp fragments of β_3 mRNA were detected at PC3, DU145, SK-OV3 cells. β-actin was used as an internal loading control. (B) Western blot for protein expression level analysis. Integrin α_V proteins were detected at all cell lines and integrin β_3 proteins were

detected at DU145 and SK-OV3 cells. β -actin was used as an internal loading control. (Protein size; integrin α_V is 135-145 kDa, integrin β_3 is 100 kDa)

In vitro level integrin $\alpha_V\beta_3$ binding of cRGDyK-HSA

To confirm integrin $\alpha_V\beta_3$ specific binding of the cRGDyK-HSA in cellular level, DBCO-HSA and cRGDyK-HSA were conjugated with fluorescence, FNR648, and visualized using confocal microscopy. There are two types of DBCO-HSA and cRGDyK-HSA in each case, the difference is the number of DBCO and cRGDyK; in case of DBCO, reaction 1 is 3.94 ± 0.70 and reaction 2 is 6.72 ± 0.41; in case of cRGDyK, reaction 1 is 2.07 ± 0.51, reaction 2 is 5.29 ± 0.76 (Table 1). After the fluorescence labeling to DBCO-HSA and cRGDyK-HSA, FNR648 labeled HSA and cRGDyK-HSA were purified with PD-10 column. At figure 4A, fluorescence labeled HSA were accumulated in cytosol and membrane, but there were no difference in reaction 1 and reaction 2. And when pre-treated excess HSA (500-fold higher amount), the accumulation in cells were decreased in all reactions. (Figure 4A). To certify cRGDyK-HSA targeting integrin $\alpha_V\beta_3$, FNR648 labeled cRGDyK-HSA (reaction 1 and reaction 2) were treated and there are two groups of confocal images; one is cells treated with only FNR648 conjugated cRGDyK-

HSA, the other is cells pre-treated with excess cRGDyK and after then treated with FNR648-cRGDyK-HSA. Reaction 1 and reaction 2 of the FNR648-cRGDyK-HSA were localized in the cell membrane and the intracellular regions. And in reaction 2 of FNR648-cRGDyK-HSA, the accumulation of FNR648 labeled cRGDyK-HSA were higher than that of in reaction 1 (Figure 4B). And in excess cRGDyK (500-fold higher) pre-treated groups, compared to FNR648-cRGDyK-HSA only treated groups, very small amount of FNR648-labeled particles were found in the cell membrane or the intracellular regions (Figure 4B). Also, the decreased amounts of cRGDyK-HSA were higher in reaction 2. Compared fluorescence labeled HSA treated groups with cRGDyK-HSA treated groups, in reaction 1, there were almost no difference in accumulation of probes. But in reaction 2, as cRGDyK were conjugated to HSA, more probes were accumulated in cells. This results demonstrate that the cRGDyK-HSA bound to integrin $\alpha_V\beta_3$ and entered the cells via integrin $\alpha_V\beta_3$-receptor-mediated endocytosis and when cRGDyK were more conjugated to

HSA, the accumulation of probes were increased by cRGDyK targeting integrin $\alpha_V\beta_3$.

A

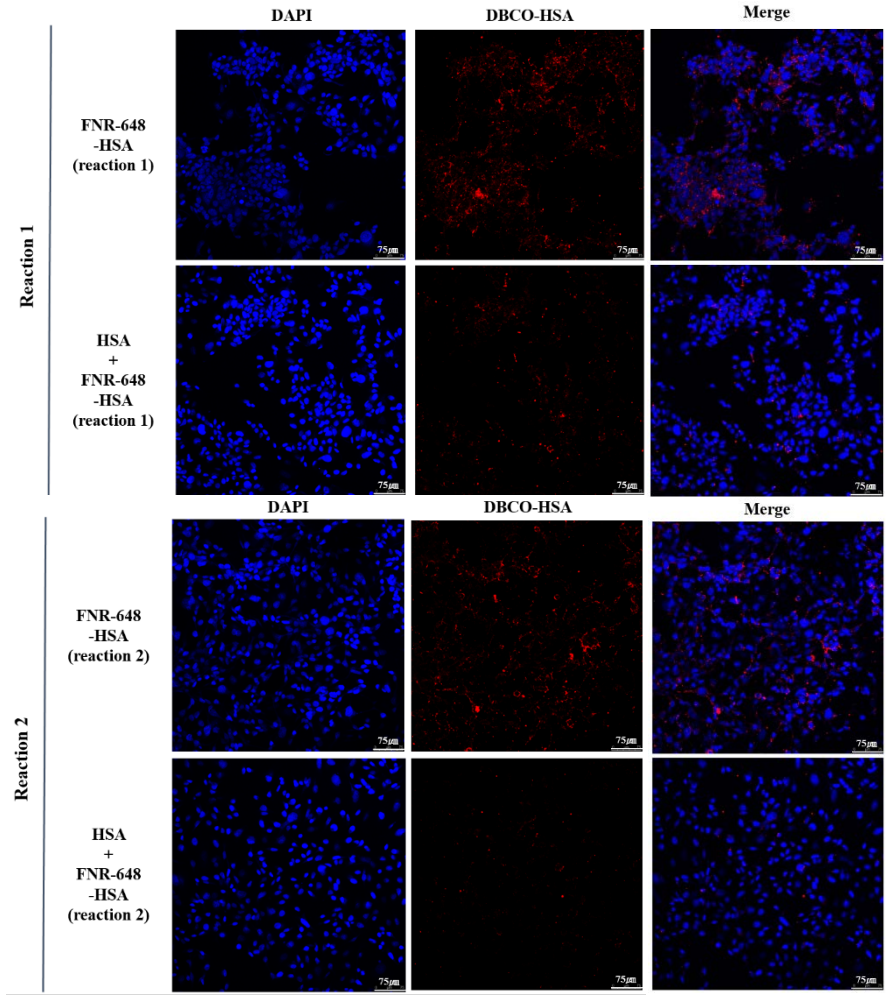
DAPI
DBCO-HSA
Merge
Reaction 1
FNR-648
-HSA
(reaction 1)
HSA
+
FNR-648
-HSA
(reaction 1)
DAPI
DBCO-HSA
Merge
Reaction 2
FNR-648
-HSA
(reaction 2)
HSA
+
FNR-648
-HSA
(reaction 2)
75μm

B

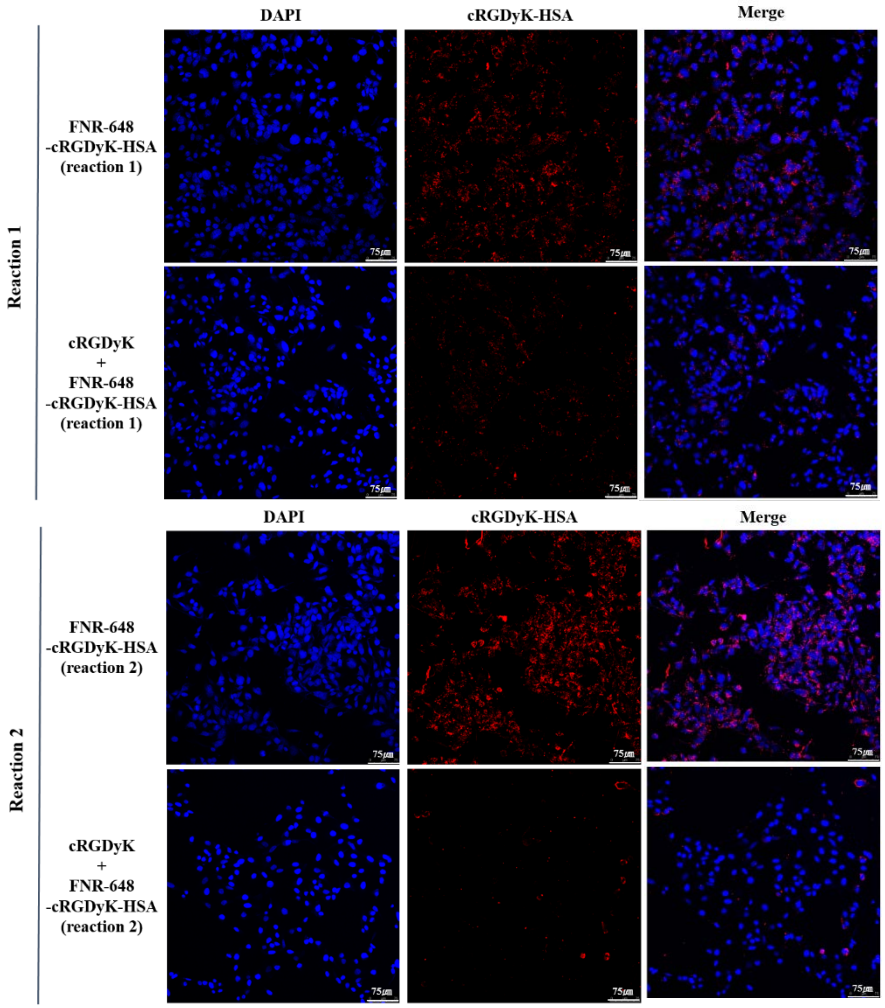
DAPI
cRGDyK-HSA
Merge
Reaction 1
FNR-648
-cRGDyK-HSA
(reaction 1)
cRGDyK
+
FNR-648
-cRGDyK-HSA
(reaction 1)
DAPI
cRGDyK-HSA
Merge
Reaction 2
FNR-648
-cRGDyK-HSA
(reaction 2)
cRGDyK
+
FNR-648
-cRGDyK-HSA
(reaction 2)
75μm

Figure 4. Cell binding and internalization of cRGDyK-HSA

(A) SK-OV3 cells were treated with fluorescence (FNR648) labeled HSA (2 nmole) for 30 minutes. To certify FNR648 labeled HSA were bound to cells by HSA, excess HSA (500-fold, 1000 nmole) were pre-treated for blocking.

(B) SK-OV3 cells were treated with FNR648 labeled cRGDyK-HSA (2 nmole) for 30 minutes. For certifying that cRGDyK-HSA is targeting integrin $\alpha_V\beta_3$, excess cRGDyK (500-fold) were pre-treated for blocking groups. In case of cRGDyK-HSA only treated groups, FNR648-labeled cRGDyK-HSA were located in cell membrane and intracellular regions. On the other hand, in cRGDyK pre-treated groups, there were very small amount of cRGDyK-HSA were observed in cells. And compared reaction 1 and reaction 2 in cRGDyK blocking, accumulation were more decreased in reaction 2. (Scale bar is 75 ㎛)

In vitro uptake of ^{64}Cu-HSA and ^{64}Cu-cRGDyK-HSA

To investigate the radiolabeled cRGDyK-HSA also specifically bind to cells, cell uptake test were conducted. ^{64}Cu labeled HSA and cRGDyK-HSA were treated to two cell lines, one is 22Rv1, which is integrin $\alpha_V\beta_3$ negative cell line, the other is SK-OV3, which is integrin $\alpha_V\beta_3$ positive cell line (Figure 3). Cells were treated with ^{64}Cu-HSA or –cRGDyK-HSA (reaction 1 and reaction 2). Cell uptake values were divided to treated source counts per minute (CPM) and changed as % values for comparing all different probes. And all values were expressed as means ± SDs of four samples. The uptake percentage of ^{64}Cu-cRGDyK-HSA in reaction 1 was 0.086 ± 0.01 % for 22Rv1 and 0.45 ± 0.06 % for SK-OV3. The uptake percentage of ^{64}Cu-cRGDyK-HSA in reaction 2 was 0.065 ± 0.017 % for 22Rv1 and 0.38 ± 0.04 % for SK-OV3. In all reaction, ^{64}Cu-cRGDyK-HSA showed higher uptake in SK-OV3 cells, integrin $\alpha_V\beta_3$ specific uptake (reaction 1, P = 0.0159 and reaction 2, P = 0.0357, Figure 5). In ^{64}Cu-HSA, two cell lines had very similar uptake percentage values (reaction 1; 22Rv1 was 0.23 ± 0.06 %, SK-OV3 was

0.24 ± 0.08 %. Reaction 2; 22Rv1 was 0.20 ± 0.12 %, SK-OV3 was 0.33 ± 0.05 %. In each reaction, compared the value of 22Rv1 and SK-OV3, $P > 0.1$), so there were no differences in ^{64}Cu-HSA uptake in these two cell lines. From this results, ^{64}Cu-labeled cRGDyK-HSA were integrin $\alpha_V\beta_3$ specifically taken up into the cells.

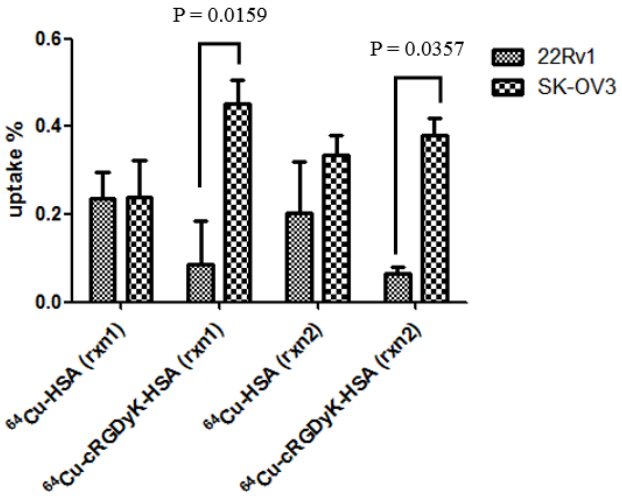

Figure 5. *In vitro* uptake test of ^{64}Cu-HSA and -cRGDyK-HSA

Uptake percentage of 22Rv1 and SK-OV3 cells. Cells were treated with ^{64}Cu labeled HSA or cRGDyK-HSA for 1 h at 37℃. The values are expressed as uptake %, each CPM values were divided by the CPM of applied radioactivity and changed as percentage value. Each values are means of four samples ± SD (N = 4). Each values (uptake percentage) were written in results paragraph.

Small animal PET imaging of ^{64}Cu-HSA and ^{64}Cu-cRGDyK-HSA

There are differences in reaction 1 and reaction 2, for example, in case of HSA, each reaction has different number of DBCO (DBCO-HSA; reaction 1 was 3.94 ± 0.70 and reaction 2 was 6.72 ± 0.41, Table 1). DBCO is linker for cRGDyK conjugation in HSA, reaction 2 have more cRGDyK than reaction 1 (cRGDyK-HSA; reaction 1 was 2.07 ± 0.51 and reaction 2 was 5.29 ± 0.76, Table 1). So, to investigate the difference in biodistribution in case of DBCO-HSA and cRGDyK-HSA or the biodistribution pattern were affected by the number of DBCO or cRGDyK conjugated to HSA, ^{64}Cu-labeled HSA and -cRGDyK-HSA (each had reaction 1 and reaction 2) were injected to tumor bearing mice (SK-OV3, integrin $\alpha_V\beta_3$ positive) via tail vein. PET images were acquired at 10 min, 4 h, 24 h, 48 h post injection (p.i.) and shown in Figure 5A. Compared to reaction 1 and reaction 2 of ^{64}Cu-HSA, blood vessels were visible to 24 h p.i. in reaction 1 and were to 4 h p.i. in reaction 2. When compared reaction 1 of ^{64}Cu-HSA and -cRGDyK-HSA, at 24 h p.i., ^{64}Cu-HSA could

recognize blood vessels but ^{64}Cu-cRGDyK-HSA could not. In case of reaction 2, blood vessels were well visible in ^{64}Cu-HSA, but not visible in ^{64}Cu-cRGDyK-HSA at 4 h p.i.. In the aspect of tumor targeting, all ^{64}Cu-HSA and –cRGDyK-HSA (reaction 1 and reaction 2), the highest accumulation in tumor were observed at 4 h p.i. and after that time point, tumor accumulation were decreased. When compared ^{64}Cu-HSA and -cRGDyK-HSA, because cRGDyK-HSA have targeting moiety, cRGDyK, ^{64}Cu-cRGDyK-HSA were more accumulated in tumor than ^{64}Cu-HSA. And the highest accumulation was observed in reaction 2 of ^{64}Cu-cRGDyK-HSA at all time points (Figure 6A and 6B). Quantification analysis in tumor also revealed reaction 2 of ^{64}Cu-cRGDyK-HSA had the highest %ID/g (% injected dose per gram) value, 5.37 $\pm$ 1.09 %ID/g, at 4 h p.i.. And at all time points, %ID/g value of ^{64}Cu-cRGDyK-HSA in reaction 2 was higher than that of others. From this results, when HSA conjugated with cRGDyK, the blood circulation time were decreased, but reaction 2 of cRGDyK-HSA can use to target integrin $\alpha_V\beta_3$ high expressing tumor.

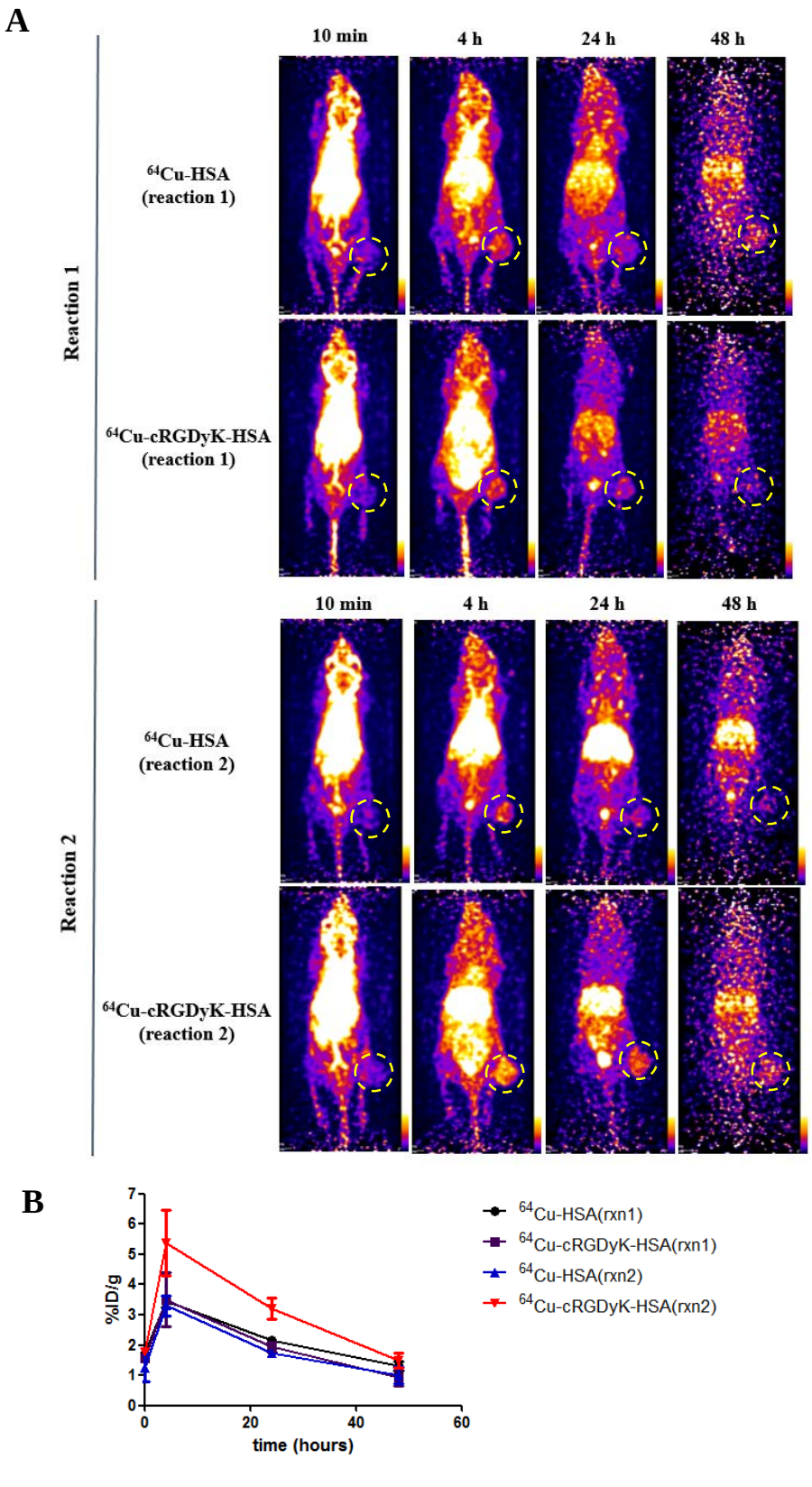
A
10 min
4 h
24 h
48 h
Reaction 1
64Cu-HSA
(reaction 1)
64Cu-cRGDyK-HSA
(reaction 1)
Reaction 2
64Cu-HSA
(reaction 2)
64Cu-cRGDyK-HSA
(reaction 2)
B
%ID/g
time (hours)
64Cu-HSA(rxn1)
64Cu-cRGDyK-HSA(rxn1)
64Cu-HSA(rxn2)
64Cu-cRGDyK-HSA(rxn2)

Figure 6. ***In vivo*** **tumor imaging of ^{64}Cu-HSA and ^{64}Cu-cRGDyK-HSA**

(A) Representative small animal PET images in SK-OV3 tumor bearing nude mice. Maximum intensity projection (MIP) images at 10 min, 4 h, 24 h, 48 h after tail vein injection of ^{64}Cu-HSA and -cRGDyK-HSA. Yellow circle indicates tumor region. (B) Time versus %ID/g curves from PET images at tumor site. Each time points %ID/g values are mean of two values ± SD (N = 2). The tumor %ID/g of ^{64}Cu-cRGDyK-HSA (reaction 2) was the highest at 4 h p.i. and was about 1.6-fold higher than that of ^{64}Cu-HSA (reaction 2).

DISCUSSION

RGD has been used in many tumor targeting imaging, to target integrin $\alpha_v\beta_3$ (7). For tumor growth more than 1-2 mm in diameter, pro-angiogenic switch on, integrin $\alpha_v\beta_3$ is overexpressed in tumors (20). But RGD is small peptides, so fast clearance through the kidney system is a problem for targeting the tumor. Aim of this study was to develop HSA-loaded cRGDyK nanoparticles for targeting tumor. By using HSA, I expected to improve the half-lives of RGD and the ability of tumor targeting. To conjugate RGD to HSA, click reaction was used in favorable condition (pH 7, 37℃).

In radiolabeling process at representative radiolabeling data (Figure 2B), cRGDyK-HSA in reaction 1 showed relatively low radiolabeling efficiencies. The 3-azidopropyl was conjugated to cRGDyK-HSA via click reaction, but the number of DBCO left to click reaction for radiolabeling was low (approximately reaction 1; 1-2, calculated from Table 1). If the number of DBCO will be increased, then DBCO will be left more for conjugating 3-azidopropyl-^{64}Cu after N_3-cRGDyK conjugation. Consider the structure of

cRGDyK, this peptide is cyclic form, cRGDyK may conceal DBCO which were left. Using the linker, such as polyethylene glycol (PEG), linker conjugated cRGDyK can have some distance from the HSA and DBCO, then radiolabeling efficiencies can be increased. Some researchers using RGD peptides with linkers, tumor targeting of RGD peptides were enhanced (21, 22, 23). Although those studies were not conjugated RGD to a carriers, using the linker conjugated cRGDyK may enhance the targeting efficiencies of cRGDyK-HSA.

There is a study about changing the number of RGD (24). In this study, there were two probes, one is dimer-RGD and the other is tetramer-RGD. When compared with dimer- and tetramer-RGD in *in vivo*, because these probes have different number of RGD, tetramer-RGD probes were more accumulated in tumors. Also, this research group also accomplished tetramer- and octamer-RGD probes imaging, to compare tumor targeting efficiencies (25). In this study, the tumor accumulation at initial time points were very similar, but when compared at later time points, octamer-RGD probes were retain their tumor

accumulation percentage, but in case of tetramer-RGD, tumor accumulation were decreased. From these papers, the number of RGD can affect the characteristics of probes and also change tumor targeting efficiency. In my paper, from PET images, reaction 2 of cRGDyK-HSA had the highest %ID/g value to tumor compared to the others (Figure 6A). So, using cRGDyK-HSA with more cRGDyK can enhance tumor targeting more efficiently or retain the accumulation of the probes at tumor. For more cRGDyK-HSA additions, conjugating more cRGDyK to HSA (for this, it maybe need more DBCO should be conjugated to HSA) and certifying there is any difference more cRGDyK in HSA for targeting integrin $\alpha_v\beta_3$ positive tumor should be accomplished.

In this study, DBCO-HSA and cRGDyK-HSA were successfully synthesized. And as the molar ratio of DBCO or cRGDyK were different, the number of conjugated DBCO or cRGDyK to HSA were consistently different. Using click reaction, ^{64}Cu was successfully labeled to HSA and cRGDyK-HSA. cRGDyK-HSA could bind to integrin $\alpha_v\beta_3$ in tumor cells and the probes were internalized to cells. And the ^{64}Cu-labeled cRGDyK-HSA were certainly

accumulated in integrin $\alpha_V\beta_3$ positive tumor cells. *In vivo* PET imaging results probed that the ^{64}Cu-cRGDyK-HSA could target tumor after 4 h p.i.. These promising results demonstrate that ^{64}Cu-labeled cRGDyK-HSA can be used as PET tumor imaging probes, which will be useful for various diagnostic applications.

REFERENCES

1. Carmeliet P, Jain RK. Angiogenesis in cancer and other diseases. Nature. 2000;407(6801):249-57.

2. Brooks PC, Clark RA, Cheresh DA. Requirement of vascular integrin alpha v beta 3 for angiogenesis. Science. 1994;264(5158):569-71.

3. Costouros NG, Diehn FE, Libutti SK. Molecular imaging of tumor angiogenesis. Journal of cellular biochemistry Supplement. 2002;39:72-8.

4. Desgrosellier JS, Cheresh DA. Integrins in cancer: biological implications and therapeutic opportunities. Nature reviews Cancer. 2010;10(1):9-22.

5. Pierschbacher MD, Ruoslahti E. Variants of the cell recognition site of fibronectin that retain attachment-promoting activity. Proceedings of the National Academy of Sciences of the United States of America. 1984;81(19):5985-8.

6. Pierschbacher MD, Ruoslahti E. Cell Attachment Activity of Fibronectin Can Be Duplicated by Small Synthetic Fragments of the Molecule.

Nature. 1984;309(5963):30-3.

7. D'Andrea LD, Del Gatto A, Pedone C, Benedetti E. Peptide-based molecules in angiogenesis. Chemical biology & drug design. 2006;67(2):115-26.

8. Yang G, Nie P, Kong Y, Sun H, Hou G, Han J. MicroPET imaging of tumor angiogenesis and monitoring on antiangiogenic therapy with an (18)F labeled RGD-based probe in SKOV-3 xenograft-bearing mice. Tumour biology : the journal of the International Society for Oncodevelopmental Biology and Medicine. 2015;36(5):3285-91.

9. Liu Z, Jia B, Shi J, Jin X, Zhao H, Li F, et al. Tumor uptake of the RGD dimeric probe (99m)Tc-G3-2P4-RGD2 is correlated with integrin alphavbeta3 expressed on both tumor cells and neovasculature. Bioconjugate chemistry. 2010;21(3):548-55.

10. Wu Y, Zhang XZ, Xiong ZM, Cheng Z, Fisher DR, Liu S, et al. microPET imaging of glioma integrin alpha(V)beta(3) expression using Cu-64-labeled tetrameric RGD peptide. J Nucl Med. 2005;46(10):1707-18.

11. He XM, Carter DC. Atomic structure and chemistry of human serum

albumin. Nature. 1992;358(6383):209-15.

12. Langer K, Anhorn MG, Steinhauser I, Dreis S, Celebi D, Schrickel I, et al. Human serum albumin (HSA) nanoparticles: Reproducibility of preparation process and kinetics of enzymatic degradation. Int J Pharm. 2008;347(1-2):109-17.

13. Gradishar WJ, Tjulandin S, Davidson N, Shaw H, Desai N, Bhar P, et al. Phase III trial of nanoparticle albumin-bound paclitaxel compared with polyethylated castor oil-based paclitaxel in women with breast cancer. Journal of clinical oncology : official journal of the American Society of Clinical Oncology. 2005;23(31):7794-803.

14. Kottschade LA, Suman VJ, Amatruda T, 3rd, McWilliams RR, Mattar BI, Nikcevich DA, et al. A phase II trial of nab-paclitaxel (ABI-007) and carboplatin in patients with unresectable stage IV melanoma : a North Central Cancer Treatment Group Study, N057E(1). Cancer. 2011;117(8):1704-10.

15. Dijkgraaf I, Liu S, Kruijtzer JA, Soede AC, Oyen WJ, Liskamp RM, et al. Effects of linker variation on the in vitro and in vivo characteristics of an 111In-labeled RGD peptide. Nuclear medicine and biology. 2007;34(1):29-35.

16. Vegt E, de Jong M, Wetzels JF, Masereeuw R, Melis M, Oyen WJ, et al. Renal toxicity of radiolabeled peptides and antibody fragments: mechanisms, impact on radionuclide therapy, and strategies for prevention. J Nucl Med. 2010;51(7):1049-58.

17. Gaertner FC, Kessler H, Wester HJ, Schwaiger M, Beer AJ. Radiolabelled RGD peptides for imaging and therapy. European journal of nuclear medicine and molecular imaging. 2012;39 Suppl 1:S126-38.

18. Jewett JC, Bertozzi CR. Cu-free click cycloaddition reactions in chemical biology. Chemical Society reviews. 2010;39(4):1272-9.

19. Sletten EM, Bertozzi CR. Bioorthogonal chemistry: fishing for selectivity in a sea of functionality. Angewandte Chemie. 2009;48(38):6974-98.

20. Folkman J. Tumor angiogenesis: therapeutic implications. The New England journal of medicine. 1971;285(21):1182-6.

21. Liu Z, Niu G, Shi J, Liu S, Wang F, Liu S, et al. (68)Ga-labeled cyclic RGD dimers with Gly3 and PEG4 linkers: promising agents for tumor integrin alphavbeta3 PET imaging. European journal of nuclear medicine and molecular

imaging. 2009;36(6):947-57.

22. Liu Z, Liu S, Wang F, Liu S, Chen X. Noninvasive imaging of tumor integrin expression using (18)F-labeled RGD dimer peptide with PEG (4) linkers. European journal of nuclear medicine and molecular imaging. 2009;36(8):1296-307.

23. Shi J, Kim YS, Zhai S, Liu Z, Chen X, Liu S. Improving tumor uptake and pharmacokinetics of (64)Cu-labeled cyclic RGD peptide dimers with Gly(3) and PEG(4) linkers. Bioconjugate chemistry. 2009;20(4):750-9.

24. Wu Y, Zhang X, Xiong Z, Cheng Z, Fisher DR, Liu S, et al. microPET imaging of glioma integrin {alpha}v{beta}3 expression using (64)Cu-labeled tetrameric RGD peptide. J Nucl Med. 2005;46(10):1707-18.

25. Li ZB, Cai W, Cao Q, Chen K, Wu Z, He L, et al. (64)Cu-labeled tetrameric and octameric RGD peptides for small-animal PET of tumor alpha(v)beta(3) integrin expression. J Nucl Med. 2007;48(7):1162-71.

국문 초록

서론: RGD는 인테그린 $\alpha_v\beta_3$를 표적으로 하는 잘 알려진 펩타이드이며, 이를 이용한 종양의 영상화는 매우 효과적이다. 그러나, RGD는 매우 짧은 체내 순환시간을 가지며 주입된 대부분이 신장이나 간담도계를 통해 빠져나간다. 본 연구에서는 RGD의 생체 내 반감기 및 종양 표적을 향상시키기 위해서, 클릭 반응을 통해 cRGDyK를 알부민에 접합시켰다. 또한 가장 적합한 RGD 접합 알부민 나노입자를 개발하기 위해서 두 가지 종류의 cRGDyK가 접합된 알부민을 합성하였고, 이 cRGDyK-알부민의 특징을 확인하였으며, 세포수준과 생체내에서 인테그린 $\alpha_v\beta_3$를 발현하는 종양을 표적화 할 수 있는지를 확인하였다.

방법: 알부민 : DBCO-NHS 에스터 물수 비율을 기준으로 반응 1번은 1 : 5.62, 반응 2번은 1: 11.24로 알부민과 DBCO-NHS 에스터를 클릭 반응을 이용해 결합시켰다. 그리고 DBCO-알부민 : N_3-cRGDyK 몰수 비율을 기준으로 반응

1번은 1 : 3, 반응 2번은 1 : 6으로 DBCO-알부민과 N_3-cRGDyK의 결합반응을 진행했다. 동위원소 표지를 위해, 방사성 구리-64가 붙은 3-azidopropyl-NOTA를 DBCO-알부민과 cRGDyK-알부민에 클릭반응을 통해 결합시켰다. 각각의 결합 반응 후에는 반응물을 인산완충생리식염수를 용매로 다공성컬럼인 PD-10을 이용해 분리했다. 모든 반응물은 질량분석기를 이용해 분석하였으며, 방사성 표지 효율은 크로마토그래피 방법으로 확인하였다. 방사성 구리-64가 붙은 알부민과 cRGDyK-알부민의 안정성을 확인하기위해, 이들 각각을 혈청과 섞어주고 시간별로 크로마토그래피로 분석하였다. cRGDyK-알부민이 인테그린 $\alpha_V\beta_3$를 세포 수준에서 표적할 수 있는지 확인하기 위해 FNR648을 붙인 cRGDyK-알부민을 공초점 현미경을 통해 영상화하였고, 구리-64가 붙은 cRGDyK-HSA로 세포 업테이크를 확인하였다. 이후 방사성 구리-64가 붙은 알부민과 cRGDyK-알부민을 종양을 가지고 있는 마우스에 정맥을 통해 투여하였으며, 소동물용 양전자단층촬영 기기를 이용하여 정맥 투여 후 10 분, 4 시간, 24 시간,

48 시간에 마우스를 영상화 하였다.

결과: DBCO-NHS 에스터와 cRGDyK는 반응시킨 몰수에 따라 성공적으로 알부민에 결합하였다. DBCO의 경우, 알부민에 붙은 DBCO의 개수는 반응 1의 경우 3.94 ± 0.70개, 반응 2의 경우 6.72 ± 0.41개였다. cRGDyK의 경우, 알부민에 붙은 cRGDyK의 개수는 반응 1의 경우 2.07 ± 0.51개, 반응 2의 경우 5.29 ± 0.76개였다. 방사성 구리-64-알부민과 cRGDyK-알부민 중 반응 2번의 표지효율은 100%였으며, cRGDyK-알부민 중 반응 1번의 경우에는 PD-10으로 분리해 낸 이후 거의 100% 표지효율을 보였다. 구리-64-알부민과 cRGDyK-알부민은 혈청과 섞어준 이후 48 시간이 지나도 안정적으로 결합하여 있는 것을 확인할 수 있었다. 공초점현미경 영상에서는, FNR648이 붙은 cRGDyK-알부민은 세포막과 세포 내 영역에 존재하였으며, cRGDyK-알부민의 500배의 cRGDyK를 우선 세포에 처리해주었을 때 cRGDyK-알부민의 이런 분포는 보이지 않았다. 구리-64가 붙은 cRGDyK-알부민의 세포내 섭취는 22Rv1 세포 (인테그린 $\alpha_v\beta_3$ 비발현)에

비해 SK-OV3 세포(인테그린 $\alpha_v\beta_3$ 과발현)에서 확연히 높았다. 양전자단층촬영 영상에서는, 구리64-알부민과 cRGDyK-알부민의 종양 섭취가 정맥 주입 후 4 시간까지 증가하였으며, 이 시간대에 cRGDyK-알부민 반응 2번이 가장 높은 종양 내 섭취를 보였다.

결론: 이 연구에서 DBCO-알부민과 cRGDyK-알부민을 성공적으로 합성하였고, 클릭 반응을 이용하여 방사성 구리-64를 알부민과 cRGDyK-알부민에 성공적으로 표지하였다. cRGDyK-알부민은 인테그린 $\alpha_v\beta_3$를 종양 세포에서 결합할 뿐만 아니라 생체 수준에서도 효과적으로 종양을 표적하는 것을 영상적으로 확인할 수 있었다. 따라서, 방사성 구리-64가 표지된 cRGDyK-알부민은 종양 영상 표적제로 사용할 수 있을 것이다.

주요어: 인테그린 $\alpha_v\beta_3$, RGD, 알부민, 생물직교 클릭 반응, 양전자 단층 촬영 영상, 구리-64

학 번: 2014-21152